JOURNAL OF GEOPHYSICAL RESEARCH, VOL. 95, NO. A11, PAGES 18,781-18,790, NOVEMBER 1, 1990

HEATING OF MINOR IONS BY THE CORONAL SLOW SHOCK

Y. C. Whang and Xuepu Zhao[1]

Department of Mechanical Engineering, Catholic University of America, Washington, D. C.

K. W. Ogilvie

Laboratory for Extraterrestrial Physics, NASA Goddard Space Flight Center, Greenbelt, Maryland

Abstract. The coronal slow shock has been predicted to exist embedded in large coronal holes at 4-10 solar radii. We use a three-fluid model to study the jumps in minor ion properties across a slow shock such as the coronal slow shock. We formulate the jump conditions in the de Hoffmann-Teller frame of reference. The Rankine-Hugoniot solution determines the MHD flow and the magnetic field across the shocks. For each minor ion species, the fluid equations for the conservation of mass, momentum and energy can be solved to determine the velocity and the temperature of the ions across the shock. We also obtain a similarity solution for heavy ions. The results show that on the downstream side of the slow shock the ion temperatures are nearly proportional to the ion masses for He, O, Si, and Fe in agreement with observed ion temperatures in the inner solar wind. This indicates that the possibly existing coronal slow shock can be responsible for the observed heating of minor ions in the solar wind.

1. Introduction

Alpha particles and other minor ions have been extensively observed since the first measurement of the solar wind. The dynamical behavior of alpha particles and other minor ions in the solar wind is not yet well understood. The helium to hydrogen abundance ratio $\epsilon = n_\alpha/n_p$ is highly variable. The long- term average value of ϵ is in the range of 0.03 to 0.06. The average value of the speed ratio, U_α to U_p, is slightly greater than 1.00. The speed ratio, U_α to U_p, near 0.3 AU is greater than that near 1 AU. The most probable value of T_α/T_p is between 3 and 4. There is a strong tendency in the solar wind for the ion temperatures to be roughly proportional to the masses [Bochsler, 1989; Bochsler et al., 1985; Hernandez et al., 1987; Marsch et al., 1982; Neugebauer, 1981; Neugebauer and Snyder, 1966; Ogilvie et. al., 1968; Ogilvie et al., 1990].

In this paper we study the jumps in flow properties for alpha particles and other minor ions across slow shocks. A few slow shocks have been identified in the solar wind [Richter, 1987], but the changes in properties of minor ions across them have not been published. Observations of changes of alpha particles' velocity, density, and temperature have been published, both for fast interplanetary shocks and for the Earth's bow shock [Borodkova et al., 1989; Fuselier et al., 1988; Neugebauer, 1970; Ogilvie et al., 1982; Zastenker et al., 1986]. Both Ogilvie et al. [1982] and Borodkova et al. [1989] reported that reacting to the presence of the cross-shock potential difference the alpha particles are decelerated less than the protons and a temperature-mass proportionality is introduced by the action of a fast shock. It has also been observed that magnetic forces contribute appreciably to the slowing of ions in the de Hoffmann-Teller frame of reference [Thomsen et al., 1987]. We expected that slow shocks and fast shocks may have similar effects on the dynamical behavior of solar wind ions. This study concludes that the possibly existing coronal slow shock can be responsible for the heating of minor ions and perhaps the variation in flow velocities for different kinds of ions in the solar wind.

The coronal slow shock has been predicted to exist embedded in large coronal holes at 4-10 solar radii [Whang, 1982]. The model considers the heliomagnetic polar regions of the Sun as the sources of solar wind streams; interplanetary magnetic fields of one polarity emanating from the north polar cap and fields of opposite polarity from the south polar cap are separated by a neutral sheet. In coronal space, the high-speed solar wind streams emanating from the polar coronal holes are sub-Alfvenic flows of low-β plasma. Studies for the expansion of the solar wind from coronal holes in rapidly diverging stream tubes indicate that supersonic speeds should be attained at points low in the corona [Kopp and Holzer, 1976; Munro and Jackson, 1977; Whang, 1983; Whang and Chien, 1978]. Streams originating from the edge of the polar open-field regions flow around the curved boundary of the helmet-shaped, closed-field region. At the edge of the neutral sheet, the flow direction of each stream changes suddenly, becoming parallel to the neutral sheet. Due to dynamical interaction in north-south direction between neighboring stream tubes, an oblique MHD slow shock can develop near the neutral point. The shock is upstream inclined, and extends poleward to form a standing coronal slow shock surrounding the Sun.

We use a three-fluid model to study the jumps in the flow properties of minor ions across slow shocks. We formulate the jump conditions in the de Hoffmann-Teller frame of reference. The Rankine-Hugoniot solution determines the MHD flow and the magnetic field across the shocks. The main body of the paper presents a three-fluid model to calculate the flow of protons and alpha particles

[1]Permanently at Department of Geophysics, Peking University, Beijing, People's Republic of China.

Paper number 90JA01232.
0148-0227/90/90JA-01232$05.00

across slow shocks under the assumptions (1) n_α is a small fraction of, but not negligible in comparison with, n_p and (2) the flow properties of electrons across slow shocks are specified by a polytropic relation. The model is also used to calculate the flow of other minor ions ($^{16}O^{6+}$, $^{28}Si^{8+}$ and $^{56}Fe^{16+}$) across slow shocks under the limits of $n_i << n_p$.

The fluid equations for the conservation of mass, momentum and energy for each kind of ion can be solved to determine the velocity and the temperature of the ions across the shock. If the protons and each kind of minor ion (k = He, O, Si, and Fe) have the same temperatures and the same velocities on the upstream side of a slow shock, then the model shows that under reasonable coronal conditions, on the downstream side of the coronal slow shock the calculated ion temperatures are nearly proportional to the ion masses and the average ion/proton velocity ratios are slightly greater than 1. Assuming that these conditions are preserved during the expansion of the solar wind between the corona and 0.3 AU, the consistent results between this study and the observations of minor ions in the inner solar wind suggest that these observations support the theoretical prediction of the existence of the coronal slow shock. We also obtain a similarity solution showing that on the downstream side of a standing slow shock the temperatures are directly proportional to masses for heavy ions.

2. Three-Fluid Model

2.1. MHD Shocks

The classical Rankine-Hugoniot relation is used to study shocks in a MHD fluid consisting of electrons, protons and alpha particles. We choose a cartesian coordinate system: the xy-plane is the plane of coplanarity, the x axis is normal to the shock surface pointing in the direction of the mass flow, and the tangential component of the magnetic field points in the positive direction of the y-axis. We formulate the flow conditions in the de Hoffmann-Teller frame of reference. Outside the shock layer, the MHD fluid velocity is aligned with the magnetic field **B**, and the electric field **E** and the non-coplanarity component of the magnetic field B_z are zero. Inside the shock layer $\mathbf{E} = E\mathbf{e}_x$, and **B**, E, and the fluid properties for each kind of particle (k = e, p and α) are functions of x only. This formulation includes a noncoplanarity component of the magnetic field inside the shock layer [Goodrich and Scudder, 1984; Gosling et al., 1988; Jones and Ellison, 1987; Thomsen et al., 1987]. The equations for the conservation of mass, momentum and energy are used to study the change in flow velocity and temperature for minor ions across the shock.

The jumps in the magnetic field **B** and the fluid properties ρ, **U**, and T outside the shock layer can be determined by the flow conditions upstream of the shock using the shock equations:

$$[\rho U_x] = 0 \tag{1}$$

$$\rho U_x[\mathbf{U}] + [P + B^2/8\pi]\mathbf{e}_x - B_x[\mathbf{B}]/4\pi = 0 \tag{2}$$

$$[U^2/2 + c_pT] = 0 \tag{3}$$

$$[B_x] = 0 \tag{4}$$

Here the pair of square brackets denote the jump of a physical quantity across the shock

$$[Q] = Q_2 - Q_1 \tag{5}$$

the subscripts 1 and 2 respectively denote the flow conditions upstream and downstream of the shock.

Whang [1987] has a simple direct method to calculate the solution of the shock equations to determine the jumps in the MHD flow and the magnetic field across oblique MHD shocks. We use this method to calculate the ratios B_2/B_1, ρ_2/ρ_1, U_{x2}/U_{x1}, and P_2/P_1 and the shock angle θ_2. (The shock angle θ is the angle between the shock normal and the magnetic field.) They are functions of three dimensionless upstream parameters: the shock Alfven number $A = U_{x1}/(a_1 \cos\theta_1)$, the shock angle θ_1, and the plasma β value. (Here a is the Alfven speed, and β the ratio of the thermal pressure P_1 to the magnetic pressure $B_1^2/8\pi$.) A shock is a slow shock if the shock Alfven number A is less than 1 and is a fast shock if A is greater than 1. The magnetic field and the shock angle decrease across a slow shock, and increase across a fast shock.

Shock solutions have been systematically studied in a three-dimensional parametric space [Edmiston and Kennel, 1986; Whang, 1988]. For given β and θ_1, shock solutions exist in the domain of $A > A_{min}$. Here the minimum shock Alfven number

$$A_{min}^2 = \{1 + 5\beta/6 - \{(1 + 5\beta/6)^2 - 10\beta\cos^2\theta_1/3\}^{1/2}\}/2\cos^2\theta_1 \tag{6}$$

for slow shocks, and

$$A_{min}^2 = \{1 + 5\beta/6 + \{(1 + 5\beta/6)^2 - 10\beta\cos^2\theta_1/3\}^{1/2}\}/2\cos^2\theta_1 \tag{7}$$

for fast shocks. Evolutionary shocks do not exist in the domain of $A < A_{min}$. There are no jumps in MHD flow properties and magnetic field when $A = A_{min}$. At any given value of β, a whole range of changes in B_2/B_1, from 0 to 1, may take place in the solution domain. The range of change in thermodynamic properties strongly depends on the β value. Slow shocks covering a wide range of jumps in thermodynamic properties (such as p and ρ) exist in the low β region ($\beta \leq 0.1$). On the other hand, only slow shocks with weak jumps in thermodynamic properties exist in the high β region ($\beta \geq 1$). Therefore, in the coronal space where the β value of the solar wind is of the order of 0.1, all physical properties may jump across a slow shock over a wide range of magnitudes. Near 1 AU the plasma β value is of the order of 1, the jumps in thermodynamic properties across a slow shock must be small but the change in the magnetic field is not necessarily small.

In place of the shock Alfven number, shock Mach number is sometimes used as an independent variable to calculate the shock relationships. The shock Mach number is defined as the ratio of U_n to the magnetoacoustic speed, C_s for slow shocks and

C_f for fast shocks. In the M,β,θ parameter space, slow shock solutions exist in the domain of

$$1 \le M^2 \le$$

$$\{1.2 + \beta + ((1.2 + \beta)^2 - 4.8\beta \cos^2\theta)^{1/2}\}/2\beta \quad (8)$$

2.2. Three Species of the MHD Fluid

We denote the three species of the MHD fluid, electrons, protons and alpha particles, respectively by subscripts e, p and α. We consider that the number density of alpha particles n_α is a small fraction of, but not negligible in comparison with the proton number density n_p. Inside the shock layer the charge density is of the order of $(h/\delta)^2 n_e e$, where h is the Debye shielding distance and δ measures the shock thickness. Since $h \ll \delta$, we may assume that to the zeroth order of magnitude

$$n_e = n_p + 2n_\alpha \quad (9)$$

In the de Hoffmann-Teller frame of reference, the electric field inside the shock layer is generated entirely by the charge separation which is a first order quantity. Now we can express the density and the flow velocity of the fluid consisting of three kinds of charged particles as

$$\rho = m_p n_p (1 + 4\epsilon) \quad (10)$$

$$U = \frac{U_p + 4\epsilon U_\alpha}{1 + 4\epsilon} \quad (11)$$

Since this study is concerned with different velocities and temperatures for alpha particle and protons, we should introduce the diffusion velocities

$$\begin{aligned} W_\alpha &= U_\alpha - U \\ W_p &= U_p - U \end{aligned} \quad (12)$$

They are respectively the velocities of alpha particles and protons in a frame of reference moving at the fluid velocity U. W_p is expected to be very small compared with W_α. Depending on the frames of reference, there are two pressure tensors for alpha particles: $(P_\alpha^*)_{ii}$ the ii component of the pressure tensor in the frame of reference moving at the fluid velocity U, and $(P_\alpha)_{ii}$ in the frame of reference moving at the flow velocity of alpha particle U_α,

$$(P_\alpha^*)_{ii} = (P_\alpha)_{ii} + m_\alpha n_\alpha W_{\alpha i}^2 \quad (13)$$

A similar relationship exists between $(P_p^*)_{ii}$ and $(P_p)_{ii}$. The fluid pressure calculated from the conservation laws is the average of the pressure tensors in the fluid frame of reference,

$$P = \frac{1}{3} \sum_i \{ (P_\alpha^*)_{ii} + (P_p^*)_{ii} + (P_e^*)_{ii} \} \quad (14)$$

On the other hand, the temperatures of alpha particles and protons are respectively defined in the frame of reference moving at flow velocities of alpha particles and protons. Namely

$$\begin{aligned} n_\alpha k T_\alpha &= \frac{1}{3} \sum_i (P_\alpha)_{ii} \\ n_p k T_p &= \frac{1}{3} \sum_i (P_p)_{ii} \end{aligned} \quad (15)$$

From these relations, we obtain that the fluid pressure

$$P = k(n_p T_p + n_\alpha T_\alpha + n_e T_e) + \frac{1}{3}(m_p n_p W_p^2 + m_\alpha n_\alpha W_\alpha^2) \quad (16)$$

In the next two subsections, we will develop a three-fluid model to calculate the flow of alpha particles across slow shocks. The equations for the conservation of mass, momentum and energy are used to calculate the change in n_α, U_α and T_α. Once we have the solutions for the alpha particles and for the MHD fluid, then we can calculate n_p, T_p, and U_p.

2.3. Lorentz Forces

Inside the shock layer, the electromagnetic field exerts a Lorentz force on each kind of charge particle (k = e, p, α),

$$L_k = Z_k n_k e E + \frac{1}{c} J_k \times B \quad (17)$$

where $Z_e = -1$, $Z_p = 1$, $Z_\alpha = 2$, and e is the elementary charge. This force and its work done on the moving plasma affect the momentum flux and the energy flux of the charged particles across the shock layer. Note that the parallel component of the electric current density makes no contribution to the Lorentz forces. We may express the Lorentz force as the sum of two parts:

$$L_k = L_k^E + L_k^M \quad (18)$$

The first part L_k^E represents the electric Lorentz force due to the electric field and the electric drift current density and second part L_k^M is the magnetic Lorentz force due to perpendicular electric current caused by the sudden change in the magnetic field configuration inside the shock layer.

We can express the Lorentz force due to the electric field and the electric drift current density as

$$L_k^E = Z_k n_k e \{E + (E \times B) \times B/B^2\}$$

or

$$L_k^E = Z_k n_k e E \cos\theta \, e_1 \quad (19)$$

where $e_1 = B/B$ is the unit vector along the field direction. Summing over all kinds of charged particles,

$$\sum_k L_k^E = 0 \quad (20)$$

This means that the electric Lorentz force produces no net effect on jumps of fluid properties for the MHD fluid, the mixture of all kinds of charged particles, as shown in the conservation equations.

Making use of Ampere's law, the sum over all kinds of charged particles of the Lorentz forces caused by the magnetic field configuration inside the shock layer must be equal to $(\nabla \times \mathbf{B}) \times \mathbf{B}/4\pi$:

$$\sum_k \mathbf{L}_k^M = (\nabla \times \mathbf{B}) \times \mathbf{B}/4\pi \qquad (21)$$

Integration of this equation over the shock layer produces the accumulated effect of the Lorentz forces which appears in the conservation equation (2). Equation (21) provides an important constraint on the magnetic Lorentz force $\mathbf{L}_k^M$. However, it is difficult to formulate the exact expression for each $\mathbf{L}_k^M$. Our scheme is to use the guiding-center theory to estimate the ratios $\mathbf{L}_e^M : \mathbf{L}_p^M : \mathbf{L}_\alpha^M$; then we can obtain a reasonably representation for each of them from (21).

The perpendicular electric current densities driven by the magnetic field configuration can be calculated from the motion of the guiding centers which are the instantaneous centers of the particle orbits. (The parallel component of the electric current density makes no contribution to the Lorentz forces.) Using the gyration theory of charged particles we can describe the effect of the changing magnetic field configuration on the motion of the guiding center. For each kind of charged particle there are three electric current densities related to the magnetic field configuration: the gradient drift current, the curvature drift current and the magnetization current. From these drift current densities, we can obtain the portion of $J_{\perp k}$ driven by the magnetic field configuration as

$$J_{\perp k} = \frac{c}{B} (P_{\parallel k} - P_{\perp k})\, \mathbf{e}_1 \times \boldsymbol{\kappa} \qquad (22)$$

where $\boldsymbol{\kappa} = \mathbf{e}_1 \cdot \nabla \mathbf{e}_1$ is the curvature vector, parallel and perpendicular subscripts refer to directions relative to the local magnetic field, $\boldsymbol{\kappa}$ points the instantaneous center of the circular arc and the radius of curvature equals $1/\kappa$. This equation shows that the perpendicular electric current density $J_{\perp k}$ ($k = p, \alpha, e$) inside the shock layer is directly proportional to the thermal pressure anisotropy $(P_{\parallel k} - P_{\perp k})$. Since the electrons are nearly thermally isotropic, our model assumes that

$$\mathbf{L}_e^M = 0 \qquad (23)$$

Based on this formulation, we can obtain an estimate for the following ratios,

$$\mathbf{L}_p^M : \mathbf{L}_\alpha^M = (P_{\parallel p} - P_{\perp p}) : (P_{\parallel \alpha} - P_{\perp \alpha}) \qquad (24)$$

From equations (21), (23) and (24) we obtain

$$\mathbf{L}_k^M = \Gamma_k (\nabla \times \mathbf{B}) \times \mathbf{B}/4\pi \qquad (25)$$

for $k = p$ and α where

$$\Gamma_p = \frac{P_{\parallel p} - P_{\perp p}}{(P_{\parallel p} - P_{\perp p}) + (P_{\parallel \alpha} - P_{\perp \alpha})} \qquad (26)$$

$$\Gamma_\alpha = \frac{P_{\parallel \alpha} - P_{\perp \alpha}}{(P_{\parallel p} - P_{\perp p}) + (P_{\parallel \alpha} - P_{\perp \alpha})} \qquad (27)$$

2.4. Jump Conditions for Alpha Particles

The equations for conservation of mass, momentum and energy for alpha particles can be integrated to give

$$[n_\alpha U_{\alpha x}] = 0 \qquad (28)$$

$$[n_\alpha m_\alpha U_{\alpha x}^2 + n_\alpha k T_\alpha] = F_\alpha \qquad (29)$$

$$[n_\alpha m_\alpha U_{\alpha x} U_{\alpha y}] = G_\alpha \qquad (30)$$

$$[U_\alpha^2/2 + 5kT_\alpha/2m_\alpha] = - Z_\alpha e[\phi]/m_\alpha \qquad (31)$$

where

$$F_\alpha = \int \{Z_\alpha n_\alpha e E \frac{B_x^2}{B^2} - \Gamma_\alpha \frac{d}{dx}(\frac{B^2}{8\pi})\}\, dx \qquad (32)$$

$$G_\alpha = \int (Z_\alpha n_\alpha e E \frac{B_x B_y}{B^2} + \Gamma_\alpha \frac{B_x}{4\pi} \frac{dB_y}{dx})\, dx \qquad (33)$$

and ϕ is the electrostatic potential. The term on the right hand side of equation (31) represents an energy sink. The alpha particles do work as they move against the electrostatic field inside the shock layer. F_α and G_α are respectively the integration of $L_{\alpha x}$ and $L_{\alpha y}$ across the shock layer. They represent the accumulated effects of the Lorentz forces over the shock layer on the momentum flux of alpha particles. The first parts of F_α and G_α show that alpha particles are decelerated by the electric Lorentz forces. The second parts of F_α and G_α represent the effects of the magnetic Lorentz forces on alpha particles. Inside a slow shock, the magnetic Lorentz forces accelerate alpha particles in the shock normal direction and decelerate alpha particles in the tangential direction. Slow shocks occur in low β plasma such as in the solar corona or in the geomagnetic tail environment. Equations (32) and (33) show that except for parallel shocks the magnetic Lorentz forces normally play a more important role than the electric Lorentz forces in affecting the dynamical behavior of alpha particles crossing slow shocks. The integrations for the z component of the momentum equations are not shown here because they only produce first order corrections to the flow speeds.

Equations (28)-(31) are used to calculate the ratios $n_{\alpha x2}/n_{\alpha x1}$, $U_{\alpha x2}/U_{\alpha x1}$, $U_{\alpha y2}/U_{\alpha y1}$ and $T_{\alpha 2}/T_{\alpha 1}$ across the shock layer. We can first use (30) to calculate the jump in tangential velocity across the shock,

$$[U_{\alpha y}] = \frac{G_\alpha}{m_\alpha n_{\alpha 1} U_{\alpha x 1}} \qquad (34)$$

Then we solve (28), (29) and (31) for $n_{\alpha x2}/n_{\alpha x1}$, $U_{\alpha x2}/U_{\alpha x1}$ and $T_{\alpha 2}/T_{\alpha 1}$. The system of equations can be reduced to a quadratic equation for $U_{\alpha x2}/U_{\alpha x1}$,

$$(U_{\alpha x2}/U_{\alpha x1})^2 - \lambda_1 (U_{\alpha x2}/U_{\alpha x1}) + \lambda_0 = 0 \qquad (35)$$

where

$$\lambda_1 = \frac{5}{4} \{ 1 + \frac{kT_{\alpha 1}}{m_\alpha U_{\alpha x 1}^2} + \frac{F_\alpha}{m_\alpha n_{\alpha 1} U_{\alpha x 1}^2} \} \qquad (36)$$

$$\lambda_0 = \frac{1}{4} - \frac{[U_{\alpha y}^2]}{4U_{\alpha x1}^2} + \frac{5kT_{\alpha 1}}{4m_\alpha U_{\alpha x1}^2} - \frac{Z_\alpha e[\phi]}{2m_\alpha U_{\alpha x1}^2} \quad (37)$$

The equation has two roots associated with the plus and minus signs of the square root term. The solution with the minus sign represents the solution of a compressive shock wave, across which the flow speed decreases and the density, pressure and entropy all increase. This step produces the most important dynamical effect of shock waves on alpha particles: part of the kinetic energy is converted to increase the thermal energy. Once we have $U_{\alpha x2}/U_{\alpha x1}$, we can calculate $n_{\alpha 2}/n_{\alpha 1}$, $T_{\alpha 2}/T_{\alpha 1}$ from

$$n_{\alpha 2}/n_{\alpha 1} = U_{\alpha x1}/U_{\alpha x2} \quad (38)$$

$$T_{\alpha 2} = T_{\alpha 1} - (m_\alpha/5k)[U_\alpha^2] - (2Z_\alpha e/5k)[\phi] \quad (39)$$

3. Results for Alpha Particles

3.1. Computational Model

Section 2 provides a theoretical formulation for the jumps in flow properties of protons and alpha particles across slow shocks. The same formulation can be used to calculate the jump of other minor ions across slow shocks (in section 4) and to calculate the jump of ions across fast shocks (in a separate paper). In order to carry out numerical computations, we need to make three further assumptions with regard to (1) the flow conditions upstream of the shock, (2) the electron flow across the shock, and (3) the thermal anisotropy of protons and alpha particles. Note that once we have a better understanding about electron flow and thermal anisotropy of ions, the theoretical formulation obtained in this paper can be upgraded to carry out new calculations.

We assume that on the upstream side of the shock all kinds of particles have the same flow velocity and the same fluid temperature,

$$T_{\alpha 1} = T_{p1} = T_{e1} \quad (40)$$

$$\mathbf{U}_{\alpha 1} = \mathbf{U}_{p1} = \mathbf{U}_{e1} \quad (41)$$

We assume that inside the shock layer the thermodynamic properties of electrons may be described by a polytropic relation

$$P_e = P_{e1}(n_e/n_{e1})^\gamma$$
$$T_e = T_{e1}(n_e/n_{e1})^{\gamma - 1} \quad (42)$$

where γ is the polytropic index ranging between 5/3 and 3 [Feldman, 1985; Schwartz et al., 1987; Scudder, 1987; Thomsen et al., 1987; Schwartz, 1988]. Computations carried out in this paper use $\gamma = 5/3$. Although the electrons carry a significant parallel electric current, the parallel electric current makes no contribution to the Lorentz forces. According to the gyration theory of charged particles, the Lorentz force induced by the magnetic field configuration on electrons is negligible because the electrons are nearly isotropic (equation (23)). In the equation of motion for electrons, the inertia term is negligible because the electron kinetic energy is much less than the electron thermal energy. The x-component of the equation of motion for electrons can be reduced to

$$\frac{dP_e}{dx} = - n_e e E \cos^2\theta \quad (43)$$

Under the polytropic law one can calculate the electrostatic potential rise across a shock from (43)

$$e[\phi] = \gamma k \langle \cos^{-2}\theta \rangle [T_e]/(\gamma - 1) \quad (44)$$

Here the pair of angle brackets denote the average value of a physical quantity inside the shock layer.

We assume that the distribution functions of the solar wind alpha particles and protons have similar asymmetries with respect to the magnetic field line. The alpha particle thermal anisotropy is generally slightly, but perhaps not significantly lower than that for protons near 1 AU [Hundhausen et al., 1970; Ogilvie et al., 1980; Marsch et al., 1982]. The ratios $P_{\parallel p}/P_{\perp p}$ and $P_{\parallel \alpha}/P_{\perp \alpha}$ can be functions of x. If we assume that $P_{\parallel p}/P_{\perp p} = P_{\parallel \alpha}/P_{\perp \alpha}$, then we can write (26) and (27) as

$$\Gamma_p = \frac{P_p}{P_p + P_\alpha} \quad (45)$$

$$\Gamma_\alpha = \frac{P_\alpha}{P_p + P_\alpha} \quad (46)$$

$P_{\parallel p}/P_{\perp p} = P_{\parallel \alpha}/P_{\perp \alpha}$ may appear as a strong assumption. We have carried out numerical solutions to show that if the two ratios differ by 20%, no visible changes can be found in the final solutions. Now, we can express the integrals for F_α and G_α in the following form:

$$F_\alpha = - Z_\alpha \left\langle \frac{n_\alpha}{n_e} \right\rangle [P_e] - \langle \Gamma_\alpha \rangle \frac{[B_y^2]}{8\pi} \quad (47)$$

$$G_\alpha = - Z_\alpha \left\langle \frac{n_\alpha B_y}{n_e B_x} \right\rangle [P_e] + \langle \Gamma_\alpha \rangle \frac{B_x[B_y]}{4\pi} \quad (48)$$

Since we do not know the detailed structure of the flow and field inside the shock layer, we have to use an approximate method to estimate those average values of physical properties which appear in (44), (47) and (48). We use the average of the values on the two sides of the shock layer to represent the average, namely $\langle Q \rangle = (Q_1 + Q_2)/2$. If Q_2 is an unknown variable of the equation system, an iteration scheme is used to calculate the average values.

We calculate the flow conditions downstream of slow shocks, with a particular interest in the two ratios $T_{\alpha 2}/T_{p2}$, and $\Delta U_\alpha/\Delta U_p$. Here ΔU_i stands for $|U_{i2} - U_{i1}|$ for i = p, α, or other minor ions. Note that the magnitude of the velocity difference ΔU_i is a quantity independent of the frame of reference. For a given combination of the plasma β value, the shock angle θ_1, and the shock Mach number or the shock Alfven number $A = U_{x1}/(a_1 \cos$

θ_1), we first calculate the ratios B_2/B_1, ρ_2/ρ_1, U_{x2}/U_{x1}, U_{y2}/U_{y1}, T_2/T_1 and θ_2 using the simple direct method of Whang [1987] for the MHD Rankine-Hugoniot relation. Then we calculate the flow conditions of alpha particles for the ratios $n_{\alpha 2}/n_{\alpha 1}$, $U_{\alpha x2}/U_{\alpha x1}$, $U_{\alpha y2}/U_{\alpha y1}$ and $T_{\alpha 2}/T_{\alpha 1}$ across the shock layer following the method developed in section 2.4 for a given initial helium to hydrogen abundance ratio $\epsilon_1 = n_{\alpha 1}/n_{p1}$. The third step is to calculate the flow conditions of protons using formulas developed in section 2.3. The solutions can be organized as functions of four dimensionless parameters: β, θ_1, ϵ_1 plus A or M.

3.2. Alpha Particles

The shock relations formulated in the de Hoffmann-Teller frame of reference have a singularity at $\theta_1 = 90°$. The iteration scheme also becomes difficult to converge for nearly perpendicular shocks. We carry out numerical solutions for $0° \leq \theta_1 \leq 60°$. For a given combination of β and ϵ_1, we can construct constant contour plots for $\Delta U_\alpha/\Delta U_p$ and T_α/T_p behind the shock on the M,θ_1 plane as shown in Figures 1 and 2. The solid lines represent the constant contours for T_α/T_p behind the shock and dashed lines for $\Delta U_\alpha/\Delta U_p$. The two panels in Figure 1 show that the variation in the helium to hydrogen abundance ratio, $\epsilon_1 = 0.05$ and 0.10, produces very insignificant changes for $\Delta U_\alpha/\Delta U_p$ and T_α/T_p behind the shock. The domain of solution for slow shocks is bounded on the right by a curve representing M = M_{max}. Slow shocks are evolutionary for $1 \leq M \leq M_{max}$. Four contour plots with varying β values are shown in Figure 2. The plasma β value has a stronger effect on the solutions of $\Delta U_\alpha/\Delta U_p$ and T_α/T_p behind the shock. The variation in β substantially changes the upper limit of the slow Mach number. As β changes from 0.01 to 0.20, M_{max} decreases from ≈11.0 to ≈2.5. At very small β, M_{max} varies as $\sqrt{(1.2/\beta)}$.

The flow parameters upstream of the coronal slow shock may be estimated to be in the range of $\beta \approx 0.02$, M > 3.0 and $15° \leq \theta_1 \leq 45°$ [Whang, 1982, Figure 1]. From Figure 2, we find that immediately downstream of the coronal slow shock the temperature ratio T_α/T_p should be in the range between 3 and 4 and the ratio U_α/U_p should be slightly greater than 1. Ion temperatures approximately proportional to the ion masses can be expected to be preserved between the corona and 0.3 AU.

4. Other Minor Ions

4.1. Computations

The three-fluid model can be used to calculate the conditions of other minor ions across a slow shock. In this case the MHD fluid consists of electrons e, protons p and a species of minor ions i = $^{16}O^{6+}$, $^{28}Si^{8+}$, $^{56}Fe^{16+}$ or others. We can assume that $n_i \ll n_p$. Under this assumption, we can use $n_p = n_e$, $\mathbf{U}_p = \mathbf{U}$, and $\Gamma_i = \langle P_i/P_p \rangle$ in the computation. Figures 3-5 shows the contour plots $\Delta U_i/\Delta U_p$ and T_i/T_p behind the shock respectively for $^{16}O^{6+}$, $^{28}Si^{8+}$ and $^{56}Fe^{16+}$ at two β values. Once again these figures show that the temperature ratio proportional to ion mass is the most important dynamical effect of a shock wave on minor ions. The coronal slow shock converts a part of the kinetic energy to increase the thermal energy. A careful examination of Figures 4 and 5 reveals a striking result that the constant contours for $\Delta U_i/\Delta U_p$ and T_i/m_i behind the shock are almost identical in these plots.

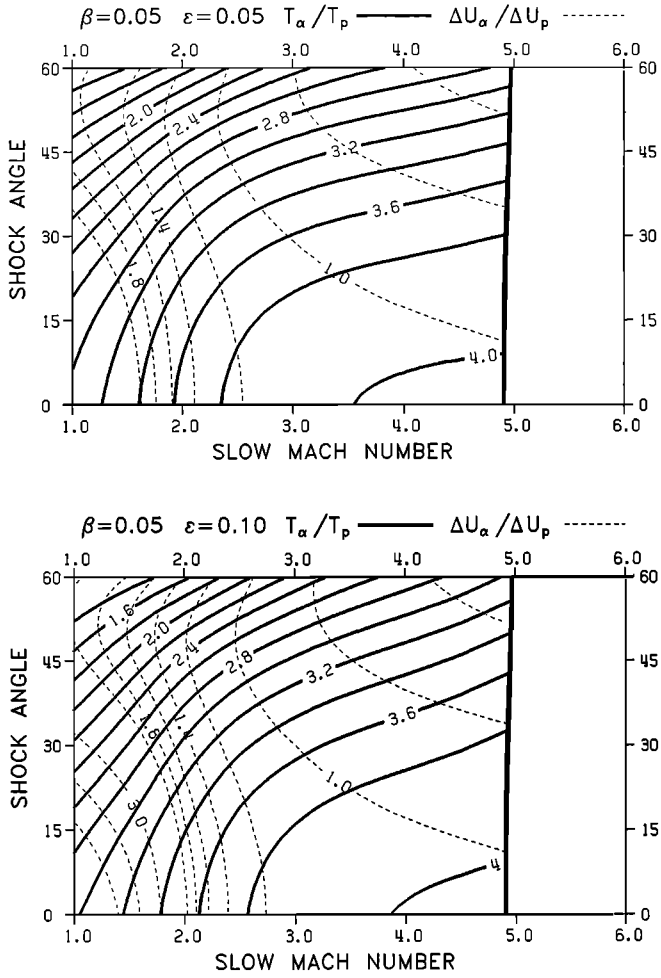

Fig. 1. Constant contours for T_α/T_p behind the shock (solid lines) and $\Delta U_\alpha/\Delta U_p$ (dashed lines). The two panels show that the variation in ϵ_1 produces very insignificant changes for T_α/T_p and $\Delta U_\alpha/\Delta U_p$.

4.2. Similarity Solutions for Heavy Ions

For heavy minor ions, because Z_i is much greater than 1, (32) and (33) show that the magnetic Lorentz force becomes less important as compared with the electric Lorentz force. Because m_i is much greater than m_p, in the upstream side of the slow shock the thermal energy is much less than the kinetic energy. If we neglect these small order terms, we can then arrange the jump conditions for heavy ions in the following form:

$$\frac{n_{i2}}{n_{i1}} U_{ix2} = U_{x1} \tag{49}$$

$$\frac{n_{i2}}{n_{i1}}\left(U_{ix2}^2 + \frac{kT_{i2}}{m_i}\right) = U_{x1}^2 + \frac{Z_i}{m_i}\int \frac{n_i}{n_{i1}} eE \frac{B_x^2}{B^2}\, dx \tag{50}$$

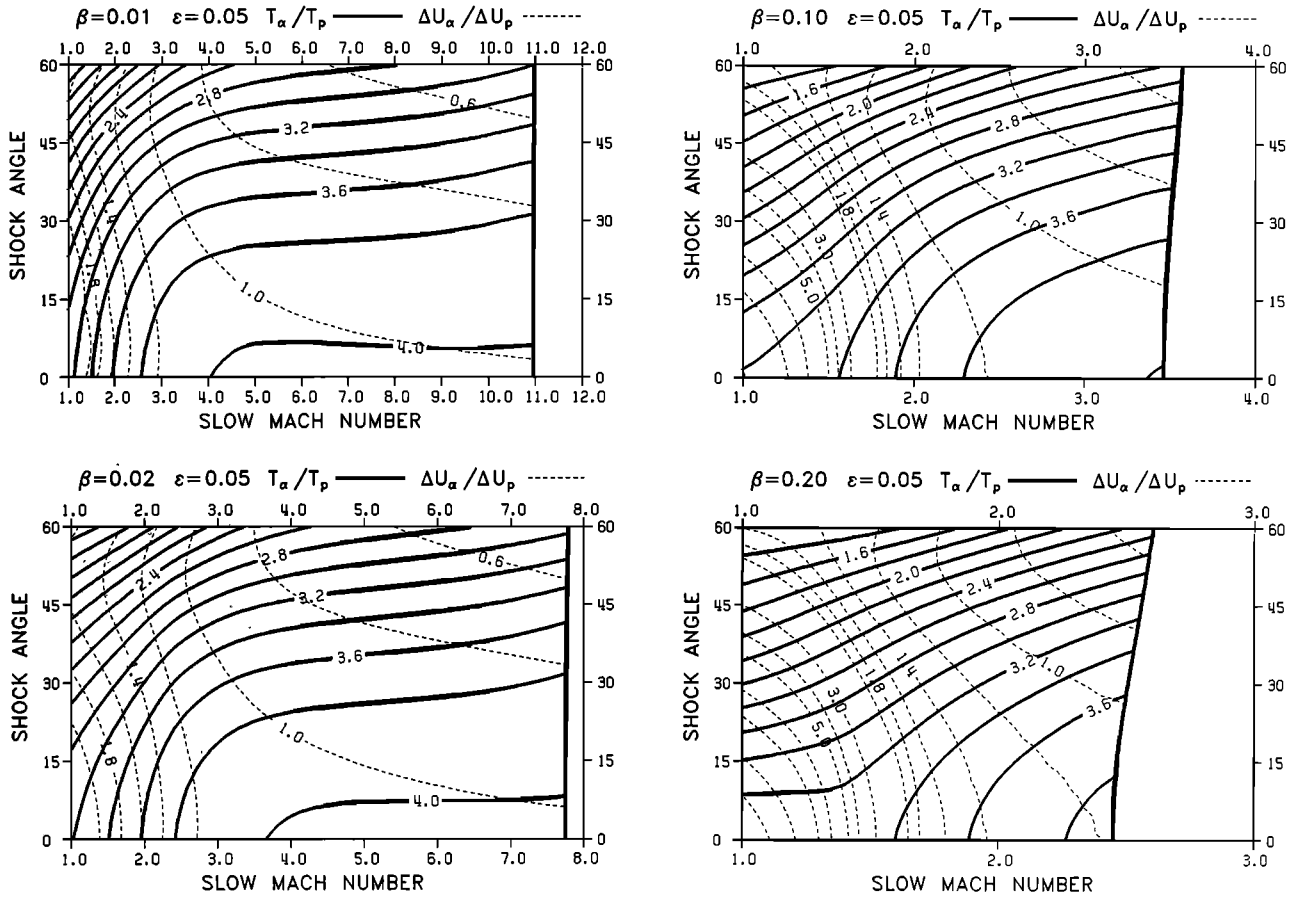

Fig. 2. Four contour plots for slow shocks with $\epsilon_1 = 0.05$ and $\beta = 0.01$, 0.02, 0.10 and 0.20 showing that the plasma β value has a strong effect on the solutions of $\Delta U_\alpha/\Delta U_p$ and T_α/T_p behind the shock.

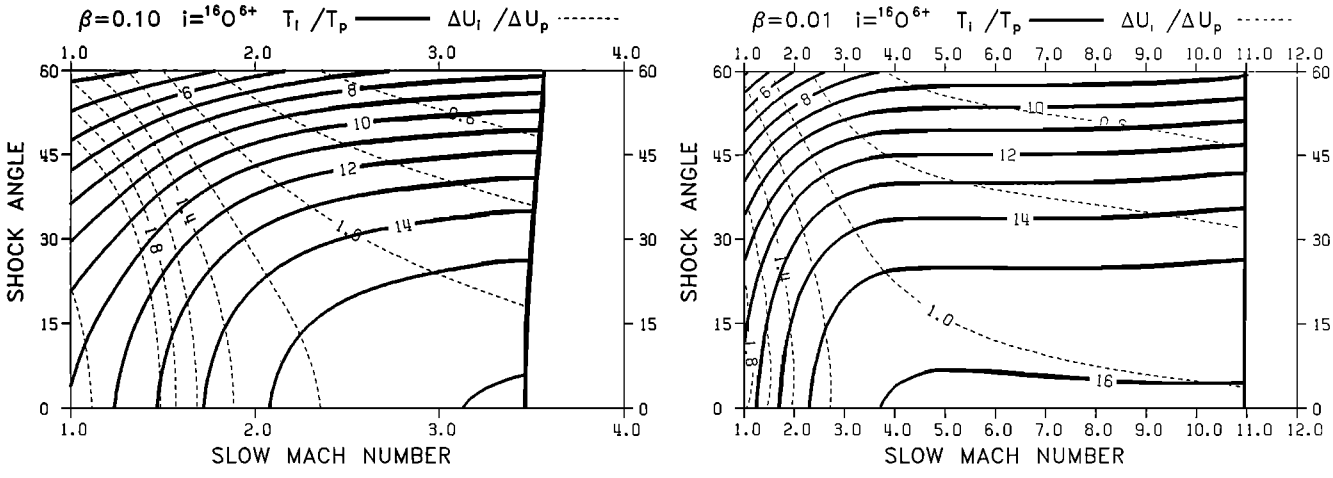

Fig. 3. From three-fluid model used to calculate the conditions of other minor ions across a slow shock, two contour plots showing the ratios $\Delta U_i/\Delta U_p$ and T_i/T_p behind the shock for i = $^{16}O^{6+}$ with $\beta = 0.01$ and 0.1.

$$\frac{n_{i2}}{n_{i1}} U_{ix2} U_{iy2} = U_{x1} U_{y1} + \frac{Z_i}{m_i} \int \frac{n_i}{n_{i1}} eE \frac{B_x B_y}{B^2} dx \quad (51)$$

$$\frac{U_{i2}^2}{2} + \frac{5}{2} \frac{kT_{i2}}{m_i} = \frac{U_1^2}{2} - \frac{Z_i}{m_i} e[\phi] \quad (52)$$

Here we have a system of four equations for four unknowns n_{i2}/n_{i1}, U_{ix2}, U_{iy2}, and kT_{i2}/m_i. In the limit of $n_i \ll n_p$, protons and electrons are responsible for the setting up of the electric field inside the shock layer and the variation of the magnetic field across the shock layer. If we consider two kinds of heavy ions having the same

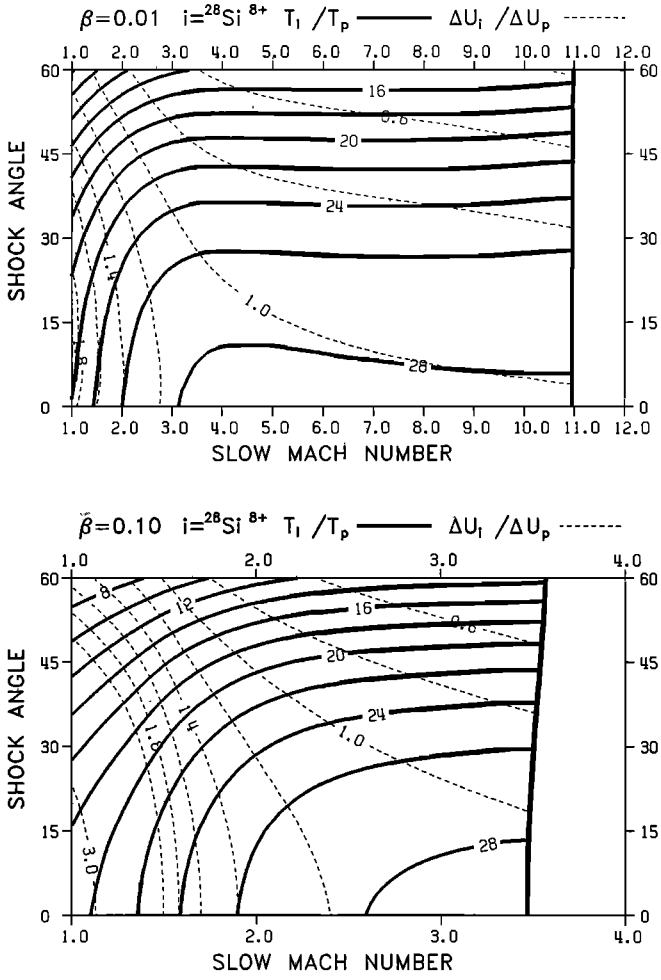

Fig. 4. Two contour plots for i = $^{28}Si^{8+}$ with β = 0.01 and 0.10. The ion temperature ratio proportional to ion mass is the most important dynamical effect of a shock wave on minor ions.

ratios Z_i/m_i across the same shock wave, the two flows are governed by the same system of four equations. All corresponding terms on the right hand sides of the two systems are identical. The two equation systems have the same solutions. The two flows are described by a set of similarity solutions, which explains why no noticeable differences exist between the computational results in Figure 4 for Si and in Figure 5 for Fe. The similarity solution for kT_i/m_i means that across the coronal slow shock the temperatures are proportional to the masses for heavy ions.

5. New Support for the Coronal Slow Shock

We use the fluid equations for the conservation of mass, momentum and energy to describe the ion flow across a reverse slow shock such as the postulated coronal slow shock predicted to occur in the low β coronal space between 4 and 10 solar radii. From Figures 1 - 5 we can see that on the downstream side of the slow shock, for He, O, Si, and Fe the ion temperatures are approximately proportional to the ion masses and the average ion velocities are slightly greater than the proton velocity. These results are consistent with the ion temperatures and velocities observed in the inner solar wind. We infer this result as a new support for the possible existence of coronal slow shocks.

If the coronal slow shock indeed exists, our understanding of the solar wind will be significantly revised. There exists one illustrative example which calculates the solar wind flow associated with the possibly existing coronal slow shocks [Whang, 1986]. The example predicts a strong latitudinal variation of the solar wind, the terminal speed at the pole being greater than that at the equator by a factor of 2 and the plasma density at the pole being less than that at the equator by a factor of 3. The support provided by this study of minor ions across slow shocks should stimulate modelers to consider the coronal slow shock in their solar wind models. A systematic study of coronal slow shocks should produce more quantitative solutions from which we can estimate the range of variation for important shock parameters such as the position and the shock strength and identify the range of coronal conditions under which coronal slow shocks may

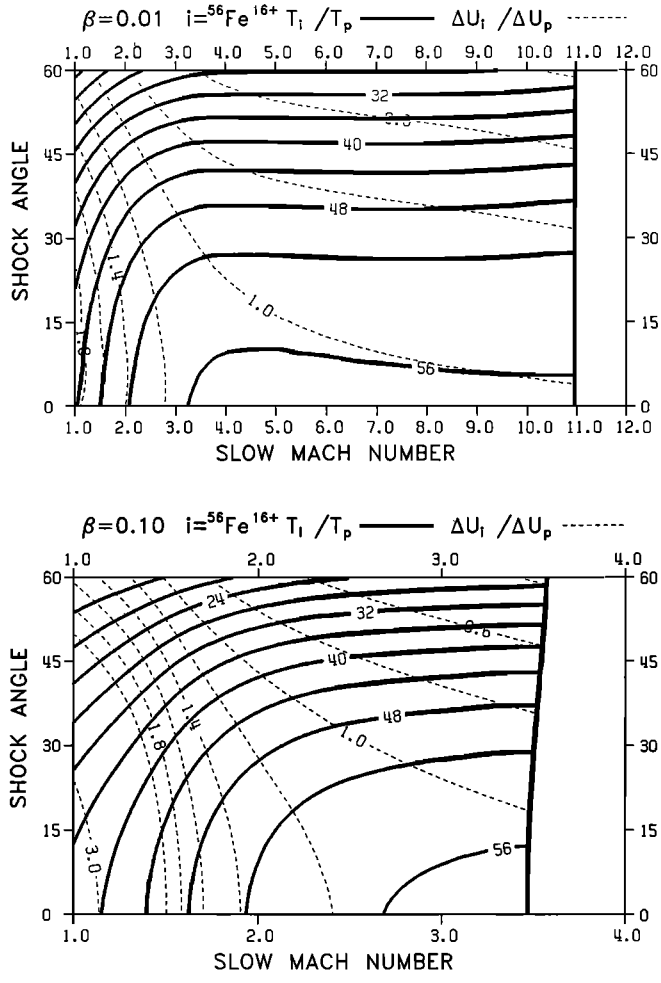

Fig. 5. Two contour plots for i = $^{56}Fe^{16+}$ with β = 0.01 and 0.10. We also obtain a similarity solution for heavy ions to explain why no noticeable differences exist between the computational results in Figure 4 for Si and in Figure 5 for Fe.

exist. Because the predicted coronal slow shock is within the reach of the future Solar Probe spacecraft, continued theoretical studies of the coronal slow shock will become very helpful in the planning of the Solar Probe mission and its experiments.

Acknowledgment. The work at the Catholic University of America was supported by National Science Foundation under NSF grant ATM-9012366 and by National Aeronautics and Space Administration under NASA grant NAGW-1323.

The Editor thanks M. Dryer and S. Livi for their assistance in evaluating this paper.

References

Bochsler, P., Velocity and abundance of silicon ions in the solar wind, J. Geophys. Res., 94, 2365-2373, 1989.

Bochsler, P., J. Geiss, and R. Joos, Kinetic temperatures of heavy ions in the solar wind, J. Geophys. Res., 90, 10,779-10,789, 1985.

Borodkova, N. L., Y. I. Yermolaev, and G. N. Zastenker, Motion of the strong disturbances in the interplanetary medium, paper presented at COSPAR Colloquium on Physics of the Outer Heliosphere, Committee on Space Research, International Council of Scientific Unions, Warsaw, September 18-22, 1989.

Edmiston, J. P., and C. F. Kennel, A parametric study of slow shock Rankine-Hugoniot solutions and critical Mach numbers, J. Geophys. Res., 91, 1361-1372, 1986.

Feldman, W. C., Electron velocity distributions near collisionless shocks, in Collisionless Shocks in the Heliosphere: Reviews of Current Research, Geophys. Monogr. Ser., vol. 35, edited by B. T. Tsurutani and R. G. Stone, p. 195, AGU, Washington, D.C., 1985.

Fuselier, S. A., E. G. Shelley, and D. M. Klumpar, AMPTE/CCE observations of shell-like He^{2+} and O^{6+} distributions in the magnetosheath, Geophys. Res. lett., 15, 1333-1336, 1988.

Goodrich, C. C., and J. D. Scudder, The adiabatic energy change of plasma electrons and the frame dependence of the cross-shock potential at collisionless magnetosonic shock waves, J. Geophys. Res., 89, 6654-6662, 1984.

Gosling, J. T., D. Winske, and M. F. Thomsen, Noncoplanar magnetic fields at collisionless shocks: A test of a new approach, J. Geophys. Res., 93, 2735-2740, 1988.

Hernandez, R., S. Livi, and E. Marsch, On the He^{2+} to H^+ temperature ratio in slow solar wind, J. Geophys. Res., 92, 7723-7727, 1987.

Hundhausen, A. J., S. J. Bame, J. R. Asbridge, and S. J. Sydoriak, Solar wind proton properties: Vela 3 observations from July 1965 to June 1967, J. Geophys. Res., 75, 4643-4657, 1970.

Jones, F. C., and D. C. Ellison, Noncoplanar magnetic fields, shock potentials, and ion deflection, J. Geophys. Res., 92, 11,205-11,207, 1987.

Kopp, R. A., and T. E. Holzer, Dynamics of coronal holes region, I, Steady polytropic flows with multiple critical points, Sol. Phys., 49, 43, 1976.

Marsch, E., K.-H. Muehlhaeuser, H. Rosenbauer, R. Schwenn, and F. M. Neubauer, Solar wind helium ions: Observations of the Helios solar probes between 0.3 and 1 AU, J. Geophys. Res., 87, 35-52, 1982.

Munro, R., and B. Jackson, Physical properties of a polar coronal hole from 2 to 5 R_o, Astrophys. J., 213, 874, 1977.

Neugebauer, M., Initial deceleration of solar wind positive ions in the Earth's bow shock, J. Geophys. Res., 75, 717, 1970.

Neugebauer, M., Observations of solar wind helium, Cosmic Phys., 7, 131-199, 1981.

Neugebauer, M., and C. W. Snyder, Mariner 2 observations of the solar wind, J. Geophys. Res., 71, 4469-4479, 1966.

Ogilvie, K. W., L. F. Burlaga, and T. D. Wilkerson, Plasma observations on Explorer 34, J. Geophys. Res., 73, 6809-6819, 1968.

Ogilvie, K. W., P. Bochsler, M. A. Coplan, and J. Geiss, Observations of the velocity distribution of solar wind ions, J. Geophys. Res., 85, 6069-6074, 1980.

Ogilvie, K. W., M. A. Coplan, and R. D. Zwickl, Helium, hydrogen, and oxygen velocities observed on ISEE 3, J. Geophys. Res., 87, 7363-7369, 1982.

Ogilvie, K. W., M. A. Coplan, P. Bochsler, and J. Geiss, Space based measurements of elemental abundances and their relation to solar abundances, Sol. Phys., in press, 1990.

Richter, A. K., Interplanetary slow shocks: A review, Proceedings of the 6th International Solar Wind Conference, Tech. Note TN-306, p. 411, Natl. Cent. for Atmos. Res., Boulder, Colo., 1987.

Schwartz, S. J., M. F. Thomsen, and W. C. Feldman, Electron dynamics and potential jump across slow mode shocks, J. Geophys. Res., 92, 3165-3174, 1987.

Schwartz, S. J., M. F. Thomsen, S. J. Bame, and J. Stansberry, Electron heating and the potential jump across fast mode shocks, J. Geophys. Res., 93, 12,923-12,931, 1988.

Scudder, J. D., The field-aligned flow approximation for electrons within layers possessing a normal mass flux: A corollary to the de Hoffmann-Teller theorem, J. Geophys. Res., 92, 13,447-13,455, 1987.

Thomsen, M. F., J. T. Gosling, S. J. Bame, K. B. Quest, and D. Winske, On the noncoplanarity of the magnetic field within a fast collisionless shock, J. Geophys. Res., 92, 2305-2314, 1987.

Whang, Y. C., Slow shocks around the Sun, Geophys. Res. Lett., 9, 1081-1084, 1982.

Whang, Y. C., Expansion of the solar wind from a two-hole corona, Sol. Phys., 88, 343-358, 1983.

Whang, Y. C., Solar wind flow upstream of the coronal slow shock, Astrophys. J., 307, 838-846, 1986.

Whang, Y. C., Slow shocks and their transition to fast shocks in the inner solar wind, J. Geophys. Res., 92, 4349-4356, 1987.

Whang, Y. C., Evolution of interplanetary slow shocks, J. Geophys. Res., 93, 251-255, 1988.

Whang, Y. C., and T. H. Chien, Expansion of the solar wind in high-speed streams, Astrophys. J., 221, 350, 1978.

Zastenker, G. N., O. Vaisberg, V. Smirnov, A. Skalsky, N. Borodkova, and Yu. Yemolavev, Solar wind protons, alphas and electrons at the bow shock and the potential barrier, paper presented at 26th meeting of COSPAR, Committee on Space Research, International Council of

Scientific Unions, Toulouse, June 30 - July 12, 1986.

K. W. Ogilvie, Laboratory for Extraterrestrial Physics, NASA Goddard Space Flight Center, Greenbelt, MD 20771.

Y. C. Whang and Xuepu Zhao, Department of Mechanical Engineering, Catholic University of America, Washington, DC 20064.

(Received March 9, 1990;
revised May 4, 1990;
accepted May 29, 1990.)